OPTIMUM INFLUENCE OF CHROMIUM AND COMBINE AUSTEMPERING-CRYOGENIC TREATMENTS ON PERFORMANCE OF DUCTILE IRON

[1,2]Idowu, A. S.*, [2]Adewuyi, B. O., [2]Folorunso, D. O., [2]Akinwekomi, A. D.

[1]Engineeering Materials Development Institute, Akure, Ondo State, Nigeria
[2]Department of Metallurgical and Materials Engineering, Federal University of Technology, Akure, Ondo State, Nigeria

*Correspondence: samsonidd@gmail.com

Abstract

The study investigates the enhancement of mechanical and tribological properties of ductile iron through differential thermal treatments and chromium alloying. Motivated by the failure of a grey cast iron screw block in a power hacksaw machine, three ductile iron compositions were produced with varying chromium additions (0%, 0.2%, and 0.3%). These were subjected to austempering and extended cryogenic treatment to assess improvements in wear resistance, tensile strength, hardness, and coefficient of friction. Results showed that ductile iron, particularly the sample with 0.2% Cr and eight-hour cryogenic treatment (hardness=334.70MPa, UTS=341.89MPa, Wear rate=8.47 mm³/N·m), outperformed other variants in all measured parameters. X-ray diffraction (XRD) analysis confirmed the presence of enhanced microstructures, including graphite nodules, pearlite, and chromium carbides, contributing to improved performance. The study revealed that such modified ductile iron is a viable replacement for grey cast iron in high-wear machine components, offering enhanced durability and reduced maintenance of machines that may breakdown as a result of worn-out spare parts.

Keywords: Ductile iron, chromium alloying, cryogenic treatment, austempering, wear resistance, power hacksaw, mechanical properties

Introduction

The need for high-performance materials with enhanced mechanical and tribological properties has significantly increased in various engineering and industrial applications, especially in the areas of machine parts, manufacturing, automotive, and mining sectors. Components subjected to high wear, such as cutting tools, gears, bearings, and machine parts, require materials with superior wear resistance to ensure long service life and reliability (Putatunda, 2001). Cast iron is a useful engineering material, which has been known in some forms for several thousand years (Alasoluyi *et al.,* 2013). It is mainly an alloy of iron, carbon and silicon with other trace elements included (Barnabas *et al.,* 2018). Grey cast iron has historically been used in applications requiring hardness and good castability (Bobba *et al.,* 2020); however, it suffers from poor toughness, impact strength and wear resistance, making it susceptible to premature failure (Yulianto *et al.,* 2025). Ductile iron, an advanced form of cast iron, has emerged as an alternative material due to its superior combination of strength, toughness, and wear resistance, making it a preferred material in applications where both impact resistance and wear resistance are required (Putatunda, 2001). However, conventional ductile iron, though superior to grey cast iron in many aspects, still faces limitations in applications requiring prolonged wear resistance and enhanced mechanical performance, especially under extreme loading conditions (Obaid *et al.,* 2024).

Wear resistance generally refers to the material's ability to resist material loss by some mechanical action, such as abrasions and frictions. Wear is one of the primary causes of material degradation in machine components operating under abrasive, adhesive, and fatigue conditions. Wear resistance in ductile iron is significantly influenced by its microstructure, matrix hardness, and the presence of alloying elements such as chromium. The wear rate, which indicates the material volume loss per unit load and distance, is a key parameter in evaluating the tribological performance of DI. A lower wear rate signifies higher wear resistance, which is

influenced by the austempering process and alloy composition (Rajan *et al.,* 2011). Wear rate, which represents the volume of material removed per unit load and distance, inversely correlates with wear resistance—the lower the wear rate, the higher the wear resistance of the material (Rajan *et al.,* 2011).

Components such as cutting tools, bearings, gears, and power hacksaw machine parts often fail due to excessive wear, leading to costly replacements and downtime (Kang *et al*., 2001). The failure of a worn screw block in a power hacksaw machine, which served as the motivation for this study, underscores the limitations of grey cast iron in high-wear applications. Grey cast iron, which has traditionally been used for such components (Zhang 2025), exhibits poor wear resistance due to its brittle nature and limited toughness. The need to replace such components frequently not only increases maintenance costs but also leads to operational downtime and inefficiencies (Singh and Dutta, 2020).

The austempering process, which involves quenching the ductile iron in a salt bath at an intermediate temperature, stabilizes the microstructure, leading to improved hardness and toughness (Singh and Dutta, 2020). In general, the ductile iron properties could be considerably enhanced through traditional heat treatment where heating, soaking and cooling are the main three parts of heat treatment process (Samar *et al.,* 2024; Vijay and Vineet, 2024).

Apart from thermal treatments, alloying elements play a critical role in enhancing the wear performance of ductile iron. Chromium is one such element that promotes carbide formation, increasing hardness and wear resistance (Geng *et al.,* 2025; Elhelaly *et al*., 2022). While chromium alloying in ductile iron has been studied extensively, there remains a gap in understanding how different chromium additions interact with differential thermal treatments, particularly the combination of austempering and cryogenic processing. This study seeks to address this gap by investigating the effects of both austempering and extended cryogenic treatment on ductile iron with varying chromium additions. Thus, improving the wear resistance of ductile iron through differential thermal treatments and alloying presents a viable solution for increasing service life and reducing maintenance-related expenses.

The need for high-performance materials with enhanced mechanical and tribological properties has significantly increased in various engineering and industrial applications, especially in the areas of machine parts, manufacturing, automotive, and mining sectors. Components subjected to high wear,

such as cutting tools, gears, bearings, and machine parts, require materials with superior wear resistance to ensure long service life and reliability (Putatunda, 2001). Cast iron is a useful engineering material, which has been known in some forms for several thousand years (Alasoluyi et al., 2013). It is mainly an alloy of iron, carbon and silicon with other trace elements included (Barnabas et al., 2018). Grey cast iron has historically been used in applications requiring hardness and good castability (Bobba et al., 2020); however, it suffers from poor toughness, impact strength and wear resistance, making it susceptible to premature failure (Yulianto et al., 2025). Ductile iron, an advanced form of cast iron, has emerged as an alternative material due to its superior combination of strength, toughness, and wear resistance, making it a preferred material in applications where both impact resistance and wear resistance are required (Putatunda, 2001). However, conventional ductile iron, though superior to grey cast iron in many aspects, still faces limitations in applications requiring prolonged wear resistance and enhanced mechanical performance, especially under extreme loading conditions (Obaid et al., 2024).

Wear resistance generally refers to the material's ability to resist material loss by some mechanical action, such as abrasions and frictions. Wear is one of the primary causes of material degradation in machine components operating under abrasive, adhesive, and fatigue conditions. Wear resistance in ductile iron is significantly influenced by its microstructure, matrix hardness, and the presence of alloying elements such as chromium. The wear rate, which indicates the material volume loss per unit load and distance, is a key parameter in evaluating the tribological performance of DI. A lower wear rate signifies higher wear resistance, which is influenced by the austempering process and alloy composition (Rajan et al., 2011). Wear rate, which represents the volume of material removed per unit load and distance, inversely correlates with wear resistance—the lower the wear rate, the higher the wear resistance of the material (Rajan et al., 2011).

Components such as cutting tools, bearings, gears, and power hacksaw machine parts often fail due to excessive wear, leading to costly replacements and downtime (Kang et al., 2001). The failure of a worn screw block in a power hacksaw machine, which served as the motivation for this study, underscores the limitations of grey cast iron in high-wear applications. Grey cast iron, which has traditionally been used for such components (Zhang 2025), exhibits poor wear resistance due to its brittle nature and limited toughness. The need to replace such components frequently not only increases maintenance costs but also leads to operational

downtime and inefficiencies (Singh and Dutta, 2020).

The austempering process, which involves quenching the ductile iron in a salt bath at an intermediate temperature, stabilizes the microstructure, leading to improved hardness and toughness (Singh and Dutta, 2020). In general, the ductile iron properties could be considerably enhanced through traditional heat treatment where heating, soaking and cooling are the main three parts of heat treatment process (Samar et al., 2024; Vijay and Vineet, 2024).

Apart from thermal treatments, alloying elements play a critical role in enhancing the wear performance of ductile iron. Chromium is one such element that promotes carbide formation, increasing hardness and wear resistance (Geng et al., 2025; Elhelaly et al., 2022). While chromium alloying in ductile iron has been studied extensively, there remains a gap in understanding how different chromium additions interact with differential thermal treatments, particularly the combination of austempering and cryogenic processing. This study seeks to address this gap by investigating the effects of both austempering and extended cryogenic treatment on ductile iron with varying chromium additions. Thus, improving the wear resistance of ductile iron through differential thermal treatments and alloying presents a viable solution for increasing service life and reducing maintenance-related expenses.

Characterization of the Worn Screw Block
The percentage Elemental composition (the Spark Test) of the Sleeve (scrap) material was obtained by using Optical Emission Spectrometer (Made in Switzerland by Thermo Fisher Scientific Sari, Model: ARL Quantodesk, Supply: 230V 50/60Hz, Phase:1, Rating 350VA, Year: 2010).

Production of Ductile Iron
Table 1 shows the composition of charge materials used to produce various ductile iron materials. Three melts of Ductile Iron were produced. The first melt has no additions of Ferrochrome; while the second and the last have little additions of Ferrochrome. Each of these were cast into a Y-Block.

Production of the first sample of ductile iron (with 0% Chromium)
Table 7The first ductile iron sample was produced using a 100 kg capacity rotary furnace. The furnace was preheated for 60 minutes before charging with 60 kg of cast iron sleeve scrap and 2 kg of graphite through the exhaust end. Graphite addition served to compensate for anticipated carbon loss during melting, thereby maintaining an optimal carbon equivalent necessary for nodularization (Stevenson et al., 2015). Following a 10-minute charging operation, the furnace was fired for 58 minutes to achieve complete melting, followed by superheating for 20 minutes to reach 1480 °C. The total heating time was 78 minutes. The molten alloy was tapped

Table 1: Composition of the Charge Materials of the Various Ductile Irons Produced

Sample	Composition				
	Cast iron (kg)	Graphite (kg)	FeSi(g)	FeSiMg(g)	FeCr(g)
1	60	2	48	752	0
2	60	2	48	752	57
3	60	2	48	752	160

Materials and Methods
The materials used to carry this research work are as listed below. , (4) ablation study, and (5) performance evaluation.

Materials
The materials that were used for this research are Grey Cast iron Scraps (Engine's sleeve), Ferro-silicon-magnesium (FeSiMg), Ferro-silicon (FeSi), Graphite, Salts (Austenitizing salts 2NaCl: 3KCl:1BaCl$_2$, Austempering salts (1NaNO$_3$: 1KNO$_3$,) and Chromium (FeCr).

Methods
The methodology applied in this research were as follows.

into a preheated ladle at 1470 °C, where it reacted with FeSiMg nodularizer for spheroidization. The magnesium-induced reaction produced mild bubbling, indicative of successful graphite nodulization (Rajan et al., 2011). After deslagging, the alloy was poured at 1454 °C into a Y-block mold precharged with FeSi inoculant to promote uniform graphite morphology and suppress carbide formation (Stefanescu, 2002). The entire melting and casting process lasted 93 minutes. Finally, the furnace was tilted downward and fired for 5minutes to remove residual slag from the shell interior for maintenance and preparation for subsequent melts (Brown and Lee, 2022).

Production of the second ductile iron sample (with 0.2% Chromium)

Following the first melt, a second batch incorporating 0.2 % chromium was prepared by charging 60 kg of cast iron sleeve scrap and 2 kg of graphite into a pre-deslagged 100 kg rotary furnace. The furnace was fired and rotated for 45 minutes to achieve uniform heating. Upon heating to 1540 °C, ferrochromium (FeCr) was introduced to the molten metal, which was subsequently superheated to 1550 °C for 10 minutes (Zhou *et al.,* 2023; Rajan *et al.,* 2011). Tapping into a ladle occurred at 1550 °C, followed by a 35-second reaction with already deposited FeSiMg nodularizer, inducing moderate turbulence typical of spheroidization reactions (Imre, 2021). After deslagging, the metal was poured into a Y-block mold containing FeSi inoculant at 1524 °C. The complete process lasted 71 minutes. Post-melt, the furnace was reheated for 5 minutes

Production of the third ductile iron sample (with 0.3% Chromium)

The third melt commenced immediately after the second, with 60 kg of cast iron sleeve scrap and 2 kg of graphite charged into the deslagged 100 kg rotary furnace. Within 35 minutes of intense heating, the charge melted at approximately 1545 °C, after which ferrochromium (FeCr) was introduced. The melt was superheated for 15 minutes and tapped at 1550 °C, making a total heating time of 50 minutes (Rajan *et al.,* 2011). Upon tapping into the ladle, where FeSiMg nodularizer was already deposited, initiating a vigorous 50-second reaction with noticeable bubbling—a typical behavior during spheroidization (Zhou *et al*., 2023). Following deslagging, the molten metal was poured into a Y-block mold at 1524°C and allowed to react with the already deposited FeSi inoculant. The final stage lasted 85 minutes in total, after which the furnace

Figure 1: Y-block As Cast Ductile Iron

Figure 2: Y-block As Cast Ductile Iron

with a downward-tilted shell to ensure thorough internal deslagging (Brown and Lee, 2022).

was fired for 5 minutes with a downward tilt to facilitate internal deslagging (Brown and Lee, 2022).

Table 2: Chemical Composition of Scrap Cast Iron (Engine Sleeve) Material

Fe	C	Si	Mn	P	S	Cr	Ni
94.58	3.500	0.0580	0.4934	0.0210	0.0305	0.1499	0.3419

Mo	Cu	Al	V	Co	Mg	Sn
0.01968	0.5997	0.005	0.0264	0.0134	0.0607	0.0597

Table 3: Chemical Composition of Cast Ductile Iron without Cr Addition

Fe	C	Si	Mn	P	S	Cr	Ni
91.08	3.614	2.2010	0.1999	0.040	0.0175	0.1476	0.1093

Mo	Cu	Ti	Nb	Co	V	W	Mg
1.525	0.2086	0.050	0.010	0.030	0.0689	0.565	0.030

Table 4: Chemical Composition of Cast Ductile Iron with 0.2 % Cr Addition

Fe	C	Si	Mn	P	S	Cr	Ni
93.05	3.502	2.262	0.2717	0.040	0.010	0.229	0.0348

Mo	Cu	Al	Ti	V	Co	Mg	Sn
0.1300	0.2111	0.025	0.0204	0.0519	0.0455	0.0753	0.010

Table 5: Chemical Composition of Cast Ductile Iron with 0.3 % Cr Addition

Fe	C	Si	Mn	P	S	Cr	Ni
92.63	3.501	2.071	0.3319	0.030	0.010	0.3021	0.0784

Mo	Cu	Al	Ti	V	Co	Mg	Sn
0.1083	0.2402	0.0159	0.0201	0.0201	0.0052	0.0365	0.0971

Fettling

The castings were allowed to cool for 72 hours naturally inside the mold before shaking out.

Preparations of Samples

From the three compositions of the cast ductile iron, standard test samples were prepared for XRD, tensile test, hardness test and wear resistance before austempering and cryogenic treatment were carried out on them.

Differential Thermal Treatment

Differential thermal treatment involves austenitisation, austempering and cryogenic treatment of the samples.

Austenitising and Austempering Process

The austenitising treatment was conducted using a neutral salt mixture comprising $2NaCl:3KCl:1BaCl_2$, melted and maintained at a temperature of 910 °C. Preheated samples were suspended on Ø14 mm rods and immersed in the molten salt bath for 1 hour to ensure complete austenitisation and homogenization of the microstructure (Rajan *et al*., 2011; Brown and Lee J, 2022).

Subsequently, the specimens were transferred directly into a nitrate-based austempering salt bath composed of a 50:50 mixture of $NaNO_3$ and KNO_3, held at 250 °C. The samples were soaked for 50 minutes to facilitate isothermal transformation into ausferrite, and then cooled in air to room temperature.

Cryogenic Treatment

Cryogenic treatment, a process of exposing materials to ultra-low temperatures to enhance mechanical properties, was performed by immersing the specimens in liquid nitrogen (−196 °C or 77 K)

contained in a Dewar flask system. In this study, standard machined samples intended for mechanical properties and XRD analysis were divided into two groups for 6-hours and 8-hours treatments, respectively.

For each treatment, 2 liters of liquid nitrogen were poured into the Dewar flask. The samples were initially suspended for 5 minutes above the liquid surface (ramp-down stage) to prevent thermal shock. They were then fully submerged and sealed within the flask to maintain a constant low temperature. After the designated cryogenic holding time (6 or 8 hours), the samples were gradually raised (ramp-up) and left to equilibrate to room temperature before further testing.

This method ensures dimensional stability and refined microstructural transformation which demonstrated improvements in mechanical properties due to deep cryogenic processing.

Hardness Test

The hardness of each sample variant was determined using a microhardness testing machine. For each composition (ductile iron with 0% Cr addition DI_0, ductile iron with 0.2% Cr addition DI_1, and ductile iron with 0.3% Cr addition DI_2) —three samples were tested, and their average hardness values were recorded.

Tensile Test

Tensile strength evaluation was conducted using a Universal Instron Tensile Testing Machine in line with ASTM standard. For each material composition (ductile iron with 0% Cr addition DI_0, ductile iron with 0.2% Cr addition DI_1, and ductile iron with 0.3% Cr addition DI_2) three samples were tested, and

the average tensile strength was recorded for analysis.

Wear Resistance Test

The wear resistance test was carried out with the aid of Tribo meter. The standard samples for the wear resistance were already machined to diameter 25mm X 6mm thickness so as to fix unto the tribometer. Hence, samples of ductile iron were mounted one after the other on the tribometer.

The wear testing machine was used to carry out the test at a speed of 10cm/s, atmospheric temperature of 27°C, and humidity of 55%. The test on the machine was carried out using a load of 5 Newton for two minutes per cycle.

The wear rate of each of the sample is calculated using Equation 1:

$$Wd = \frac{V}{FnL}\left(\frac{M^2}{N}\right) \tag{1}$$

where: W_d is Wear rate of the disc sample, V is Volume $= \frac{M}{Dm}$, M is Initial mass, Dm is $m_2 - m_1$, m_1 is Initial mass of the disc sample, m_2 is Final mass of the disc sample, L is distance traveled (by the rotation of the wear edge of the machine), Here L is 40 meters, Fn is 5 Newton.

Three samples from each materials composition (DI_0, DI_1, DI_2,) were run for the wear resistance test and the average was taken.

X ray Diffraction (XRD)

The X-ray Diffractometric analysis of the various samples were taken by the use of the Rigaku Phenom Prox, machine (Model: MiniFlex 600-C. Input: AC100-240V 1 phase 50/60Hz 11A. Serial No: BD69000266-01).
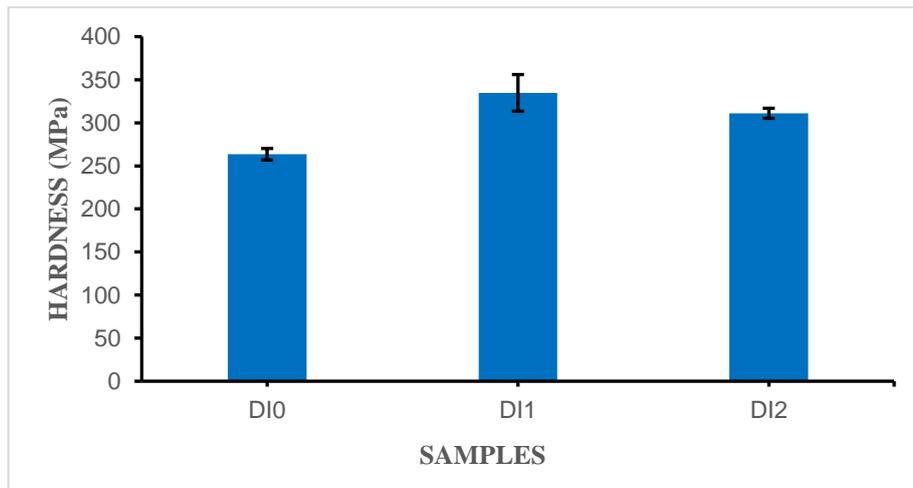

Figure 3: Hardness values of the developed ductile iron with varying compositions

The confusiwn allows a clearer view of how well the model is distinguishing between different UAV signals categories (legitimate UAV signal, jammed or compromised UAV signal and noise signals). The confusion matrix provides insights be model's detection capability under different kinds of JA scenarios is comprehensively provided by this performance evaluation.

Results and Discussion
Composition and Mechanical Properties of Screw Block and Cast Samples
Table 2 shows chemical composition of scrap cast iron (engine sleeve) material and Tables 3 to 5 show the chemical compositions of the cast ductile irons.

Table 2 shows the chemical composition of scrap cast iron (engine sleeve) material (which was the fundamental material charged into the furnace and melted with some additives in order to produce the various compositions of the ductile iron). It has Fe content of 94.58% and C content of 3.50 %; which is typical of cast iron. Also, Mg is 0.0607% and the Cr content is 0.1499 %.

Table 3 shows the chemical composition of cast ductile iron without Cr addition. It is characterized with Fe content of 91.08%, C of 3.614%, Cr of 0.1476% which happened to be the least out of all the compositions; because FeCr was not added to the charge during the melting operation. It is also lesser than the Cr content in the scrap metal. This came into being because some of the Cr content in the scrap metal got burnt off as a result of heat in the furnace during melting operation. Mg content is 0.030%.

Table 4 shows the chemical composition of cast ductile iron with 0.2 % Cr addition. It has Fe content of 93.05 %, C of 3.502%, Mg content is 0.0753% and Cr of 0.229%. This Cr content is higher than the percentage in the scrap metal (Cr content of 0.1499 %) as a result of the FeCr (57g as seen in Table 1) which was added during the melting operation.

Table 5 shows the chemical composition of cast ductile iron with 0.3 % Cr addition. It shows that Fe has a composition of 92.63 %, C has 3.501%, Mg 0.0365 and Cr 0.3021. The increment in the chromium content is as a result of the added FeCr (160g as seen in Table 1) while the increment in the Mg content is as a result of FeSiMg (752g as seen in Table 1) which was added during the melting operation.

Hardness
Figure 3 presents various measurements and properties of hardness values for different samples of ductile iron (DI_o, DI_1, DI_2) compositions.

Hardness is an essential mechanical characteristic of ductile iron (DI) that affects its ability to perform in a variety of applications (Anupam *et al.*, 2024).

Ductile iron: The hardness value of 263.50MPa is recorded for the ductile iron (without Cr addition) while the value increased to 334.70MPa for the 0.2% Cr addition and later reduced to 311.0 MPa for the 0.3% Cr addition. This reduction in hardness value is due to the fact that ductile iron contains spheroidal graphite, which reinforces the matrix and provides greater resistance to deformation, resulting in higher hardness. Chromium affects the distribution and morphology of these graphite nodules. However, with higher Cr content, degeneration of nodules or promote carbide formation at the nodule-matrix interface occur resulting to weakening the matrix and reducing hardness.

The addition of ferroalloys like ferrochrome in ductile iron further enhances these properties, making it more durable and harder. The added
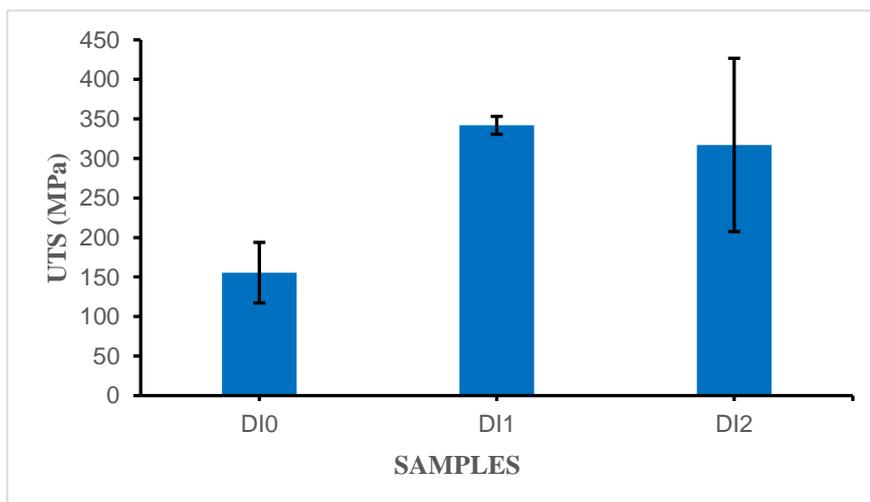

Figure 4: Ultimate Tensile Strength of the developed ductile iron with varying compositions

chromium is an alloying element that has a strong affinity for carbon, thus forming chromium carbides such as Cr_7C_3 and Cr_3C_2. These carbides are extremely hard and are dispersed throughout the matrix, acting as hard particles that resist deformation. It significantly boosts hardness. Further, its atoms dissolve into the iron matrix, distorting the lattice and impeding dislocation movement. This mechanism increases the base hardness of the ferrite or pearlite matrix even before heat treatment.

Effect of cryogenics in ductile iron samples refined the microstructure for enhanced mechanical properties and transform retained austenite into martensite. Martensite is harder contributing directly to increased hardness.

Ultimate Tensile Strength (UTS)
Figure 4 presents various measurements and properties of ultimate tensile strength values for different samples of ductile iron (DIo, DI_1, DI_2) compositions.

Ductile iron (DI0, DI1, DI2): The Ductile iron material (DI0) has a UTS of 155.47 MPa, DI1 has 341.89 MPa and DI2 317.07 MPa. The reason why all these samples have better UTS can be attributed to the presence of graphite nodules in them. These noodles tend to act against forces of dislocation when shear forces are applied to them. The noodles came into being as a result of the nodulariser (FeSiMg) that was added to the melt during casting operation. Another reason is the alloying element (FeCr) that was added to melts (DI1 and DI2) during casting operation. However, it was noticed that the UTS for the DI1 was higher than that of DI0 because DI0 has no Cr addition while DI1 has 0.2% FeCr additions during the casting operation. The trend of the UTS decreased with the 0.3% FeCr content

addition in DI_2.

Addition of chromium encourages pearlite formation over ferrite. This increases the strength but reduces ductility. Chromium increase the UTS of the ductile iron by refining the microstructure and promoting the formation of harder phases like pearlite or bainite. Its additions influence the volume fraction of ferrite and bainite. A balanced ferrite-bainite structure tends to improve tensile strength and toughness.

Cryogenics treatment converts some of the retained austenite into martensite, which is harder and increase the UTS. Also, fine carbides precipitate during cryogenic soaking, most especially in alloyed ductile irons. These carbides impede dislocation movement, boosting tensile strength stronger. This transformation also reduces dimensional instability under load.

Wear rate ($\times 10^{-7}$) mm³/N·m and wear resistance
Figure 5 presents various measurements and properties of wear rate for different samples of ductile iron (DIo, DI_1, DI_2) compositions.

Ductile iron: The ductile iron without chromium addition exhibited a wear rate of 9.2465×10^{-7} mm³/Nm, indicating relatively lower wear resistance. This can be attributed to the presence of a predominantly ferritic-pearlitic matrix, which provides limited hardness and load-bearing capacity. The soft ferrite phase tends to deform under contact stress, leading to higher material loss during sliding wear (Singh *et al.*, 2018).

With the addition of 0.2% chromium, the wear rate reduced to 8.49×10^{-7} mm³/Nm, demonstrating an improvement in wear resistance. The beneficial effect of chromium is primarily due to its ability to
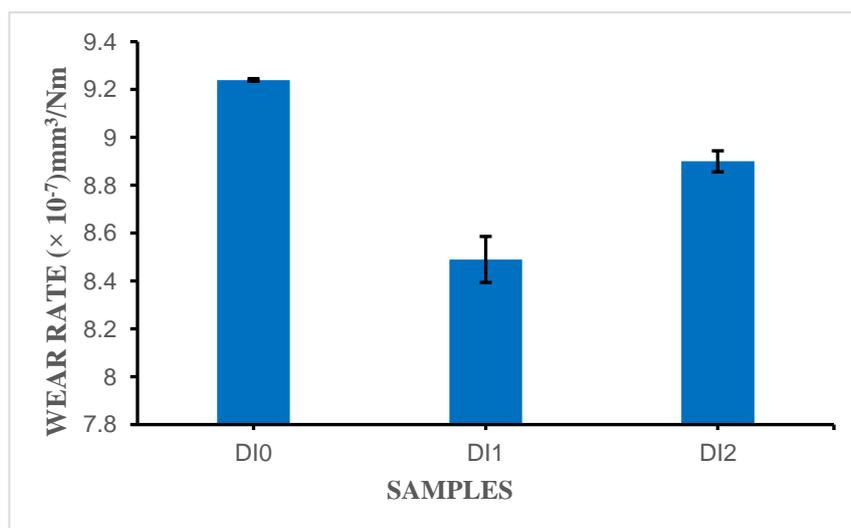

Figure 5: Wear rate of the developed ductile iron with varying compositions
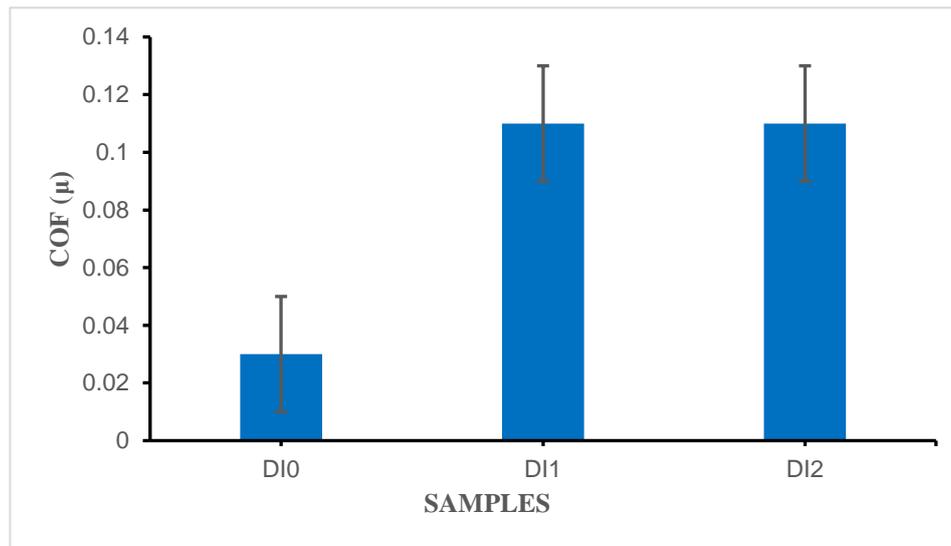
Figure 6: Ultimate Tensile Strength of the developed ductile iron with varying composition

refine the pearlitic matrix and promote carbide formation, increasing surface hardness and reducing plastic deformation during wear (Bochnowski and Gołombek, 2020).

For the ductile iron with 0.3% chromium addition, the wear rate was recorded as 8.90×10^{-7} mm³/Nm, which is slightly higher than that of the 0.2% chromium variant but still lower than the unalloyed ductile iron. This suggests that while chromium improves wear resistance, excessive addition may lead to carbide precipitation at grain boundaries, which can increase brittleness and reduce toughness (Kiani-Rashid and Elliott, 2009).

Chromium alloying leads to a more refined and homogeneous microstructure, reducing weak points where wear can initiate. The modified layer resists micro-cutting and plowing during sliding contact. It promotes the formation of hard chromium carbides (e.g., Cr_7C_3), which act as wear-resistant phases. Cr can influence the morphology and distribution of graphite nodules, indirectly affecting wear behavior.

Cryogenics leading to extreme cooling rate refines grain boundaries and reduces internal stresses, leading to a more stable and uniform wear response in the ductile iron samples. Cryogenic soaking promotes the formation of fine carbides, especially in the alloyed ductile irons. These carbides act as barriers to wear, resisting micro-cutting and plowing. This reduces surface damage during sliding or abrasive contact thus giving the materials an enhanced wear resistance.

Coefficient of Friction (μ)
Figure 6 presents various measurements and properties of coefficient of friction for different samples of ductile iron (DIo, DI$_1$, DI$_2$) compositions.

The coefficient of friction (COF) is a crucial parameter in assessing the tribological behavior of materials. It is a critical parameter in evaluating the wear behavior of materials under tribological conditions. A lower COF generally indicates reduced frictional resistance and, in some cases, improved wear performance due to minimized surface interactions (Hutchings and Shipway, 2017). However, the correlation between COF and wear resistance is complex and depends on factors such as material hardness, microstructural composition, and the formation of protective tribolayers during wear (Gahr, 2008).

While a lower COF can be advantageous in reducing energy dissipation during friction, it does not necessarily indicate superior wear resistance, as wear rate is influenced by other microstructural factors such as matrix hardness and the stability of the tribolayer (Suresh *et al.,* 2003).

Ductile iron: The ductile iron without chromium addition exhibited a COF of 0.03, which is significantly lower than that of the chromium-alloyed variants. This reduced COF is likely attributed to the presence of a relatively higher fraction of soft graphite nodules, which act as solid lubricants and facilitate smooth sliding between the contacting surfaces (Ribeiro *et al.*, 2016).

With the addition of 0.2% chromium, the COF increased to 0.11, suggesting an increase in frictional resistance. This increase is likely due to the formation of hard chromium carbides (Cr_7C_3 and Cr_3C_2) within the matrix, which improve hardness but also contribute to increased asperity interactions at the wear interface (Rajan *et al.*, 2011).

The ductile iron with 0.3% chromium addition also exhibited a COF of 0.11, indicating that further chromium addition does not significantly influence friction behavior beyond a certain threshold. The tribological response in this composition is likely dominated by the interplay between hard carbides and retained austenite, where an optimal balance of hardness and toughness is necessary to achieve effective wear resistance (Sivaprasad *et al.,* 2017). However, excessive chromium may lead to the formation of coarse carbides, (Zhao *et al.,* 2020).

The increase in COF with chromium addition can be linked to the effect of chromium in refining the microstructure, leading to a harder and more wear-resistant matrix. Studies have shown that the addition of alloying elements such as chromium enhances carbide formation, which influences frictional behavior by increasing surface roughness and adhesion between the contact surfaces (Johnson and Lee, 2019**).**

Wear Rate versus Coefficient of Friction
Wear rate versus coefficient of friction in differential thermally treated ductile irons
The tribological performance of various ductile iron samples subjected to differential thermal treatments was evaluated through measurements of wear rate ($\times 10^{-7}$ mm³/N·m) and coefficient of friction (COF, μ), as presented in Figure 7. The figure compares various compositions of differential thermally treated ductile iron with varying chromium contents (DI_0, DI_1, DI_2).

Ductile iron contains spheroidal graphite, which acts as a natural solid lubricant. Cryogenic treatment refines the matrix around these nodules, enhancing their lubricating effect. This contributes to a lower and more stable COF**.**

Impact of Chromium Addition in As-Cast Ductile Irons
The addition of 0.2% and 0.3% Cr in ductile iron (DI_1 and DI_2) resulted in progressive reductions in wear rate compared to DI_0, although not significantly. The COF remained low (~0.1–0.2), which indicates enhanced tribological performance due to the solid solution strengthening effect of Cr and possible formation of carbide precipitates $(Fe,Cr)_3C$. Similar effects were observed in the work of Jiaojiao *et al.,* (2022), who reported improved wear behaviour in Cr-alloyed cast irons due to secondary hard phase formation.

Chromium alloying reduces the coefficient of friction, further lowering wear rates and improving tribological performance. Chromium alloying reduces friction, which directly lowers wear rate and heat generation during operation.

X Ray Diffraction (XRD)
XRD of Ductile Iron (As Cast) without Chromium Addition: The XRD pattern of the as-cast ductile iron without chromium additions reveals the presence of several phases, which are characteristic of the microstructure of ductile iron.

Peak corresponding to the ferrite phase (α-Fe) are observed at 2θ angles of approximately 44.7°. These peaks are indicative of the body-centered cubic (BCC) structure of ferrite, which is a common constituent in the matrix of ductile iron (Kumar *et al.,* 2019). The presence of ferrite contributes to the toughness of the material.

The XRD pattern also reveals peaks associated with the pearlite phase, which is a lamellar mixture of
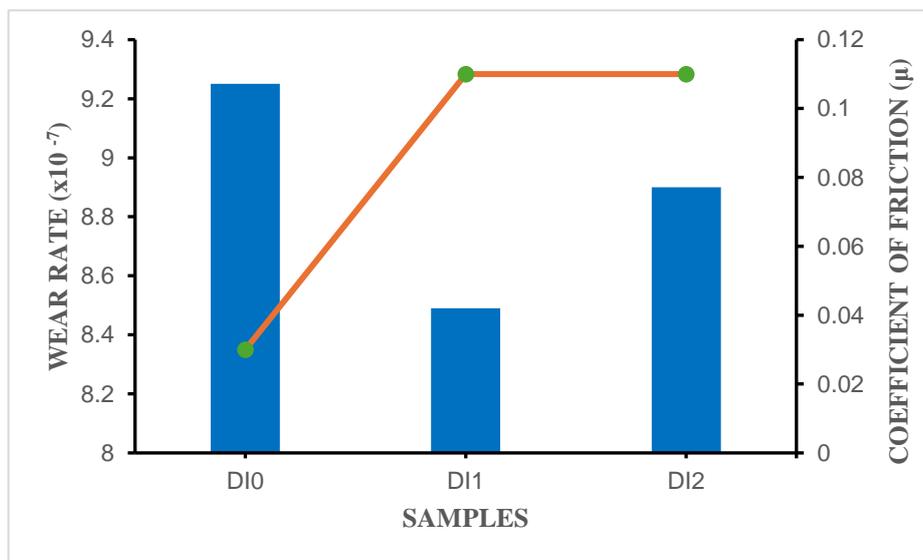

Figure 7: Chart of Wear Resistance versus Coefficient of Friction of the developed ductile iron with varying compositions
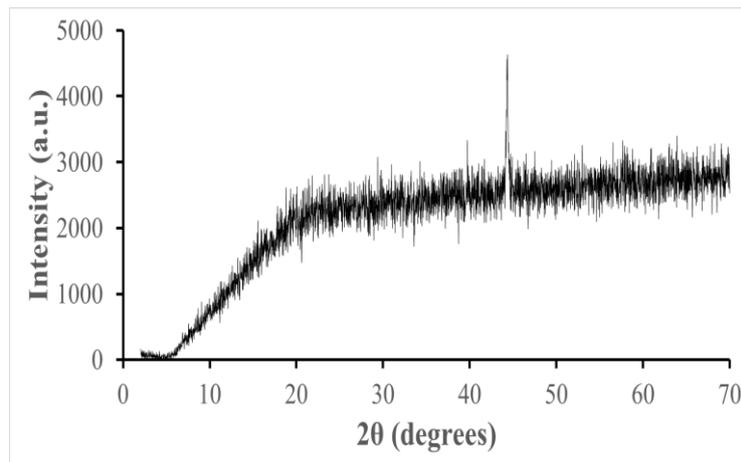
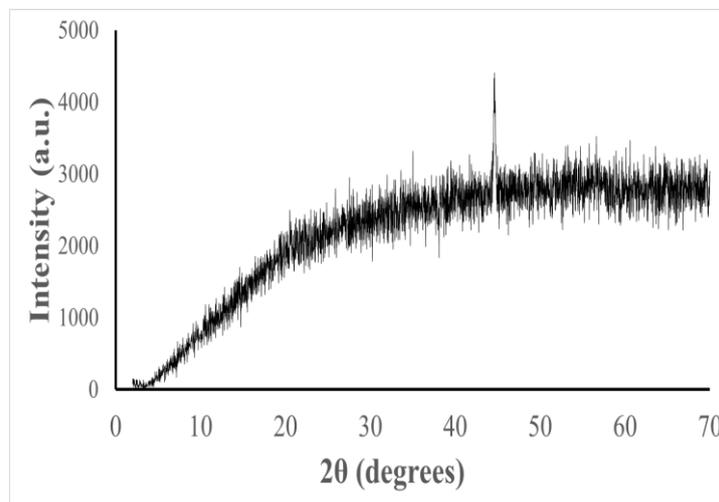**Figure 8**: XRD of Ductile Iron (As Cast) without Chromium Addition

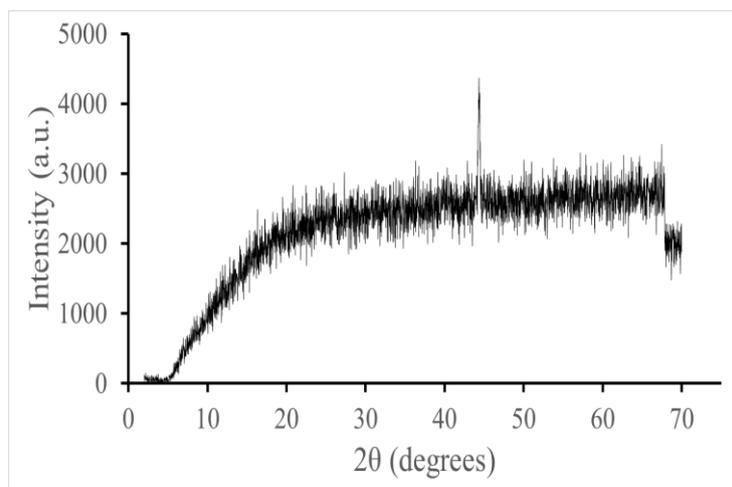**Figure 9**: XRD of Ductile Iron with 0.2% Cr Addition

Figure 10: XRD of Ductile Iron with 0.3% Cr Addition

ferrite and cementite (Fe3C). These peaks are observed at 2θ angles of approximately 45.9°, consistent with the orthorhombic structure of cementite (Singh *et al.,* 2020). The presence of

pearlite enhances the strength and hardness of the ductile iron.

Minor peaks corresponding to the austenite phase (γ-Fe) are observed at 2θ angles of approximately 43.6°. These peaks are indicative of the face-centered cubic (FCC) structure of austenite, which may be present in small amounts due to incomplete transformation during cooling (Wang *et al*., 2021).

XRD of Ductile Iron with 0.2% Cr Addition: The XRD pattern of ductile iron with 0.2% chromium additions reveals the presence of several phases, which are characteristic of the microstructure of ductile iron with alloying elements**.** The relative intensities of the peaks suggest that the microstructure is predominantly composed of ferrite and graphite, with smaller amounts of pearlite, chromium carbides, and austenite. This phase distribution is typical of ductile iron with chromium additions and is consistent with the enhanced mechanical properties.

The XRD pattern shows distinct peaks corresponding to the graphite phase, which is a primary component of ductile iron. The intensity of these peaks indicates a significant volume fraction of graphite nodules in the microstructure.

Peaks corresponding to the ferrite phase (α-Fe) are observed at 2θ angles of approximately 44.7°. These peaks are indicative of the body-centered cubic (BCC) structure of ferrite, which is a common constituent in the matrix of ductile iron (Kumar *et al*., 2019). The presence of ferrite contributes to the ductility and toughness of the material.

The XRD pattern also reveals peaks associated with the pearlite phase, which is a lamellar mixture of ferrite and cementite (Fe_3C). The presence of pearlite enhances the strength and hardness of the ductile iron.

The addition of 0.2% chromium leads to the formation of fine chromium carbides (Cr_7C_3 and Cr_2C_6) within the matrix. The presence of these carbides significantly enhances the hardness and wear resistance of the material.

Minor peaks corresponding to the austenite phase (γ-Fe) are observed at 2θ angles of approximately 43.6° and 50.8°. These peaks are indicative of the face-centered cubic (FCC) structure of austenite, which may be present in small amounts due to incomplete transformation during cooling (Li *et al.,* 2022). The presence of austenite can influence the mechanical properties, particularly in terms of toughness and fatigue resistance.

XRD of Ductile Iron with 0.3% Cr Addition: The XRD pattern of ductile iron with 0.3% chromium additions reveals the presence of several phases, which are characteristic of the microstructure of ductile iron with alloying elements.

The relative intensities of the peaks suggest that the microstructure is predominantly composed of ferrite and graphite, with smaller amounts of pearlite, chromium carbides, and austenite.

The XRD pattern shows distinct peaks corresponding to the graphite phase, which is a primary component of ductile iron. The presence of graphite is confirmed by the peaks, which are consistent with the hexagonal structure of graphite. The intensity of these peaks indicates a significant volume fraction of graphite nodules in the microstructure.

There are other peaks which are indicative of the body-centered cubic (BCC) structure of ferrite, which is a common constituent in the matrix of ductile iron. Peaks corresponding to the ferrite phase (α-Fe) are observed at 2θ angles of approximately 44.7° and 68.0°. The presence of ferrite contributes to the ductility and toughness of the material (Kumar *et al.,* 2019).

The XRD pattern also reveals peaks associated with the pearlite phase, which is a lamellar mixture of ferrite and cementite (Fe_3C). The presence of pearlite enhances the strength and hardness of the ductile iron (Singh *et al.,* 2020).

The addition of 0.3% chromium leads to the formation of fine chromium carbides (Cr_7C_3 and Cr_2C_6) within the matrix. These carbides are identified by peaks at 2θ angles of approximately 37.6° and 43.8°, which are consistent with the orthorhombic and cubic structures of chromium carbides, respectively (Wang *et al*., 2021). The presence of these carbides significantly enhances the hardness and wear resistance of the material.

Minor peaks corresponding to the austenite phase (γ-Fe) are also noticed. These peaks are indicative of the face-centered cubic (FCC) structure of austenite, which may be present in small amounts due to incomplete transformation during cooling. The presence of austenite can influence the mechanical properties, particularly in terms of toughness and fatigue resistance (Li *et al*., 2022).

Conclusion
The optimization of ductile iron through chromium addition with combined austempering and cryogenic treatment have demonstrated significant improvements in mechanical and wear-resistant properties. These treatments particularly, eight-hours cryogenically treated samples with 0.2% chromium additions, resulted in superior performance characteristics with the optimum mechanical properties. There is enhanced tensile strength and hardness due to the transformation of

the matrix into ausferrite and the formation of martensite during cryogenic treatment. Improved wear resistance was attributed to microstructural refinement, increased carbide precipitation, and reduced retained austenite is noticed.

References

Alasoluyi J.O., Omotoyinbo J. A., Olusunle S.O.O. and Adewoye O.O. (2013): Investigation of the Mechanical Properties of Ductile Iron Produced from Hybrid Inoculants Using Rotary Furnace, International Journal of Science and Technology, 2(5), 388-393.

Anupam K., Gautam S. L., Putane S. R. R. and Manali G. (2024): Enhancing Hardness Characterization in Austempered Ductile Iron with Jellyfish Swarm-Adaptive Hybrid Adaboost Approach, Nanofabricated Materials for Optical Communication and Intelligent Manufacturing, 20(3). 13-26.

Barnabas A.A., Oyetunji A. and Seidu S.O. (2018): Carbidic Austempered Ductile Iron an off-Spring of cast iron for production of agricultural implement: a review, Journal of Environmental Science and Technology, 11(6), 10-16.

Bobba S., Rao M. S., Babu B. H., and Leman Z. (2020): Effect on the mechanical properties of grey cast iron with variation of molybdenum and as-cast alloying elements. Universal Journal of Mechanical Engineering, 8(6), 298–304.

Bochnowski W, and Golombek K. (2020): Influence of Chromium on the microstructure and properties of austempered ductile iron, Materials Science and Engineering, 792, 139-145.

Brown K., and Lee J. (2022): Microstructural evolution and wear characteristics of chromium-alloyed ductile iron. Metallurgical Science and Engineering, 59(2), 99-112.

Dorazil E. (1991): High Strength Austemperd Ductile Iron. Ellis Horwood.

Elhelaly M.A., El Zomor M.A., Attia M.S., & Youssef A.O. (2022): Characterization and Kinetics of Chromium Carbide Coatings on AISI O2 Tool Steel Performed by Pack Cementation, Journal of Materials Engineering and Performance, Springer Nature, 32, 365- 375.

Gahr K. H. Z. (2008): Microstructure and wear of materials. Elsevier, 12(3), 47-59.

Geng Z., Zhang M., Zhu J., Peng Y., Zhang W. and Liu F. (2025): Effect of Chromium Carbide Addition on the Microstructures and Properties in Dual Carbide Phases Reinforced Ni Based Composite Coatings by Plasma Cladding, Materials (Basel) MDPI, 16(13), 354-365.

Hutchings, I. M., and Shipway, P. H. (2017): Tribology: Friction and wear of engineering Materials, Butterworth-Heinemann. 10, 25-40.

Imre K. (2021): Comparative Study on the In Ladle Treatment Techniques for Nodulizing the Iron's Graphite, Tehnički Glasnik, 15(4), 504–509.

Jiaojiao B., Haifeng X., Yuhui W., Xingpin C., Xiao dan Z., Wenquan C. and Yang X. (2022): Microstructures and Mechanical Properties of Ductile Cast Iron with Different Crystallizer Inner Diameters, Crystals, 12(3), 413-528.

Johnson T. and Kumar S. (2019): Retained austenite stabilization and friction control in austempered ductile iron: Cryogenic treatment effects, Journal of Materials Processing and Performance, 50(6), 500-515.

Kang Y.J., Oh J.C. and Lee H.C. (2001): Effects of carbon and chromium additions on the wear resistance and surface roughness of cast high speed steel rolls, Metallurgical and Materials Transactions A, 32, 2515–2525.

Kiani-Rashid A. R. and Elliott R. (2009): Effect of chromium on microstructure and mechanical properties of austempered ductile iron, Materials Science and Technology, 25(2), 234–240.

Kumar S., Singh R. and Gupta P. (2019): Microstructural Characterization of As-Cast Ductile Iron, Materials Today: Proceedings, 16(4), 1234–1241.

Kumar S., Singh R. and Gupta P. (2019): Microstructural Characterization of Ductile Iron with Chromium Additions, Materials Today: Proceedings, 16(4), 131–140.

Kumar S., Singh R. and Gupta P. (2019): Microstructural Characterization of As-

Cast Austempered Ductile Iron. Materials Today: Proceedings, 16(4), 1234–1241.

Lim S. C., Oh K. H. and Jang J. (2003): Tribological properties of grey cast iron under dry and lubricated conditions, Tribology International, 36(4), 233-241.

Obaid, A. Y., AlSamarai, R. A., Ahmed, S. R., & Al-Douri, Y. (2024): The effect of hardening techniques on wear resistance and fatigue life of ductile cast iron. Journal Teknologi (Sciences & Engineering), 86(2), 348-353.

Putatunda S.K. (2001): Development of austempered ductile iron: A review. Materials and Manufacturing Processes, 16(1), 1-17.

Putatunda S. K., Panneerselvam S., and Alshwigi M. (2015) : Development of nanostructured austempered Ductile cast iron (ADI), 28th ASM heat treating society conference.

Rajan T. V., Sharma C. P. and Sharma A. (2011): Heat Treatment: Principles and Techniques (2nd Edition), PHI Learning Private Limited, New Delhi, First Edition, 10-11.

Ribeiro T. A. C., Da S., Marcelo B. and Baptista, A. M. (2016): Influence of graphite morphology on the tribological behavior of cast irons. Wear, 368-369, 186–194.

Samar R. A., Haytham E. and Adel N. (2024): A comparative study of laser Fluence effect on surface modification and hardness profile of austempered ductile iron, ELSEVIER: Journal of Materials Research & Technology, 31, 3189-3204.

Singh K., Kumar S. and Prakash S. (2018): Influence of microstructure on wear behavior of ductile iron under dry sliding conditions. Journal of Tribology, 140(3), 31-46.

Singh A., Patel V. and Kumar R. (2020): XRD Analysis of Austenite in Austempered Ductile Iron. Materials Characterization, 168, 110-124.

Singh A., Patel V. and Kumar R. (2020): XRD Analysis of Pearlite in Ductile Iron. Materials Characterization, 168, 567-579.

Singh R. and Dutta N.K. (2020): Enhancing wear resistance of ductile iron using alloying and heat treatment techniques, Journal of Tribology, 142(9), 91-107.

Sivaprasad S., Chakraborti P. C. and Ghosh M. (2017): Carbide precipitation and its effect on the wear behavior of austempered ductile iron, Journal of Materials Science, 43(9), 2953-2960.

Stevenson E. P., Gladman W. B. and Guy A. G. (2015): Foundry Practice, Industrial Press / ASM International, First Edition, 15-16.

Suresh S., Sundararajan G. and Gnanamoorthy R. (2003): The effect of graphite morphology on the unlubricated wear behavior of cast iron, Wear, 255(7-12), 1153–1163.

Suresh S., Vasudevan M. and Seshadri S. K. (1998): Effect of graphite morphology on the wear behavior of cast irons." Wear, 219(1), 98-104.

Vijay K. Y. and Vineet K. T. (2024): Effect of Austempering and Martempering on Mechanical Properties and Structure of Bearing Steel, Scholars Journal of Engineering and Technology, 2(1), 76-85.

Yulianto A., Anggono A. D., Partono P., and Ngafwan. (2025): Investigation of thickness effects on cooling rate and hardness of gray cast iron in metal and sand molds. Engineering Proceedings, 84(1), 73-85.

Zhang P., Li, S., Pang X., and Lin, P. (2025): Microstructure, simulation, and wear resistance of grey cast iron with varying microhardness combination processed by bionic laser technology. Journal of Iron and Steel Research International. 16(2), 121–132.

Zhao J., Hu Y. and Liu X. (2020): Influence of carbide morphology on the tribological performance of chromium-alloyed cast iron. Materials & Design, 191(1), 108-119.